

Humidity and Wetting Effects in Spin-Cast Blends of Insulating Polymers and Conducting Polyaniline Doped with DBSA

Jakub Haberko,¹ Andrzej Bernasik,¹ Wojciech Łuzny,¹ Magdalena Hasik,² Joanna Raczowska,³ Jakub Rysz,³ Andrzej Budkowski³

¹AGH University of Science and Technology, Faculty of Physics and Applied Computer Science, 30-059 Krakow, Poland

²AGH University of Science and Technology, Faculty of Materials Science and Ceramics, 30-059 Krakow, Poland

³M. Smoluchowski Institute of Physics, Jagiellonian University, 30-059 Krakow, Poland

Correspondence to: J. Haberko (E-mail: haberko@fis.agh.edu.pl)

ABSTRACT: In this article, morphological structures are presented that are formed during spin coating of thin composite polymer films, containing a conjugated polymer. The system under study is a mixture of electrically conductive polyaniline doped with dodecylbenzenesulfonic acid and a conventional, nonconducting polymer—polystyrene or poly(methyl methacrylate). The dopant strongly influences film morphology, acting as a surfactant at a polymer/polymer interface. The effect of solution composition, spin-coating atmosphere, and solvent on final morphology is analyzed. Experimental data were collected by means of several techniques: dynamic Secondary Ion Mass Spectrometry, Atomic Force Microscopy, UV–Vis spectroscopy, and optical microscopy. © 2012 Wiley Periodicals, Inc. *J. Appl. Polym. Sci.* 000: 000–000, 2012

KEYWORDS: polymer blends; thin films; atomic force microscopy; conjugated polymers

Received 21 April 2011; accepted 18 March 2012; published online 00 Month 2012

DOI: 10.1002/app.37742

INTRODUCTION

Polyaniline doped with dodecylbenzenesulfonic acid [PANI(DBSA), Figure 1(a)] is a conjugated polymer which is easily dissolved in some organic solvents, as described by Cao et al.¹ This good processability along with relatively high conductivity (σ) of this material means that it may find numerous and diverse applications. The polymer, its composites, and derivatives have, for instance, been utilized in fabrication of polymer electronic devices, such as chemical sensors,^{2–5} supercapacitors,⁶ or photovoltaic devices.^{7,8} Other applications include shielding from electromagnetic radiation,^{9,10} construction of polymeric varistors,¹¹ or corrosion protection of steel.¹² A dispersion containing PANI(DBSA) has also been used as paint for inkjet printing of microstructures for electronic and other applications.^{13,14} The authors of this article manufactured thin PANI(DBSA) films of relatively high conductivity. The values reported by Haberko¹⁵ ranged from 0.3 S/cm for a film of approx. 300 nm thickness to $\sigma = 7.2$ S/cm in case of a 5- μm thick film. These measurements were performed via the two-point technique between a pair of gold electrodes evaporated onto glass substrate. Österholm et al.¹⁶ prepared films of PANI(DSBA) with

conductivity ranging 100 S/cm. In this instance, emulsion polymerization was carried out with DBSA acting as both a surfactant and a dopant. A value of 3.7 S/cm has been reported by Han et al.¹⁷ for PANI(DBSA) nanoparticles. Furthermore, highly conductive composites containing PANI(DBSA) were manufactured by Su and Kuramoto¹⁸ and Soares et al.¹⁹ Such high-conductivity values can be explained in terms of conformation of PANI(DBSA) molecules. If the conformation is straight, the neighboring benzene rings in a PANI macromolecule are not twisted with respect to each other. Consequently, polarons can be delocalized along a macromolecule, resulting in enhanced charge transfer and high conductivity. In case of PANI(DBSA), straight conformation is induced by steric interactions of long alkyl chains of the acid, which protonate neighboring imine groups.

Mechanical properties of conjugated polymers are usually poor. This is partially owing to the aforementioned straight conformation of a conjugated polymer backbone, necessary to achieve high electrical conductivity. One way to enhance these properties is to mix a conjugated polymer with a conventional one. The most prominent methods to prepare conducting polymer

© 2012 Wiley Periodicals, Inc.

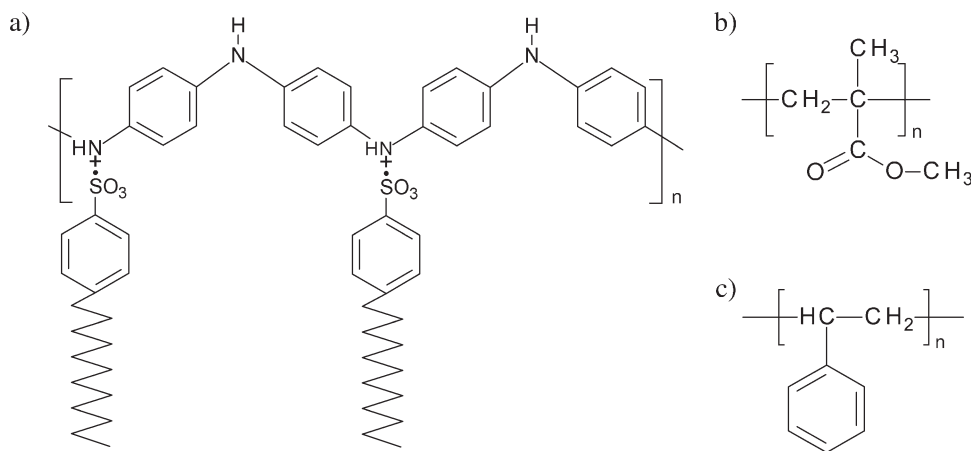


Figure 1. Structural formula of (a) PANI(DBSA), (b) PMMA, and (c) PS.

blends include electrochemical polymerization, *in situ* polymerization, melt mixing, and solvent mixing.²⁰ The latter technique is especially useful, as it allows, for instance, fabricating a polymer electronic device in only one facile production stage of spin coating. However, the film morphology is one of the most important factors influencing the performance of such devices. For example, horizontal phase separation taking place during composite film formation can be utilized to produce a field-effect transistor, as shown, for example, by Chua et al.²¹ The efficiency of polymer light-emitting diodes is also a function of film morphology. Corcoran et al.²² have shown that films with horizontal phase separation exhibit much higher quantum efficiency than the ones with lateral phase separation. Also, in the case of PANI(DBSA) mixed with polystyrene (PS) for sensing purposes, morphology of the final material plays an important role, as shown by Segal et al.²³ In this instance, morphology influences the sensor's sensitivity and reproducibility. A significant factor influencing conductivity of a blend is the dispersion of the conducting PANI(DBSA) phase in the insulating matrix. This problem has been addressed by Vicentini et al.²⁴ for PANI(DBSA)/thermoplastic polyurethane composites. Recently, there have also been successful attempts to manufacture nanocomposites of PANI(DBSA) and reduced graphene oxide.²⁵ The resulting films possessed favorable mechanical properties and enhanced electrical conductivity with respect to bare PANI(DBSA) films. Reduced graphene oxide was finely dispersed in the polymer matrix, the morphology of the sample being very uniform.

In this article, morphological structures in polymer blends containing PANI(DBSA) mixed with a conventional polymer are studied. We focus on the influence of manufacturing process details, such as solution composition, spin-coating atmosphere, and others, on the final film morphology. The host polymers of choice are PS and poly(methyl methacrylate) (PMMA). PS is a thermoplastic polymer with the density between 1.04 and 1.13 g/cm³, exhibiting high thermal stability and very high resistivity (10²⁰–10²² Ω cm). The latter renders it an excellent insulating material. Its dielectric constant equals approx. 2.5. It is soluble in many nonpolar organic solvents (benzene, cyclohexane, chloroform, xylene, and others) and insoluble in polar solvents. PMMA is also a good electrical insulator and has the dielectric

constant of approx. 3.3. It is soluble in alcohols and insoluble in most nonpolar solvents. It is transparent in the visible range and almost transparent in the UV, down to approx. 260 nm. PMMA and PS have similar tensile moduli (approx. 3 GPa) and tensile strengths (48–76 and 30–60 MPa for PMMA and PS, respectively). Good mechanical as well as insulating properties of these polymers render them suitable candidates for matrix materials in blends containing conjugated polymers, such as PANI(DBSA).

EXPERIMENTAL

The following procedure was applied to prepare polymer solutions: PANI powder (emeraldine base, purchased from Sigma-Aldrich, St. Louis, MO, $M_w = 5$ kDa) was added to isopropanol solution of dodecylbenzenesulfonic acid (70% wt., Sigma-Aldrich, St. Louis, MO). The ratio of dopant to polymer was 0.5 acid molecule per 1 nitrogen atom in a PANI macromolecule. Isopropanol was then added and the solution was mixed for 24 h to allow enough time for protonation of PANI. Following that, the solution was spilled onto a large glass vessel and dried under low vacuum (20 kPa, 70°C) for 24 h. Dark green deposit left on the bottom of the vessel after drying was sticky, the effect which could not be eliminated neither by elongating the drying time nor by raising the temperature. It testifies to the fact that only partial protonation of PANI took place and that the sediment contains some amount of free DBSA, not chemically bound to PANI. Full protonation of PANI is hindered by steric interactions of polymer with DBSA alkyl chains. In the next step, the sediment was removed from the vessel, mixed with a solvent (xylene or chloroform), and stirred for another 24 h. Further on, it was filtered through a teflon Whatman Puradisc 25 TF filter and a matrix polymer was added (PS, $M_w = 125$ kDa or PMMA, $M_w = 14.4$ kDa, both purchased from PSS Mainz, Germany). The final solution was filtered again. Thin films were prepared by spin coating ($\omega = 1000$ –3000 rpm) onto a monocrystalline Si wafer, covered with a thermally evaporated gold layer of approx. 100 nm. The spin-coater chamber was either blown with Ar to generate dry atmosphere or filled with water vapor, which resulted in relative humidity of >90%. In some cases, the conventional polymer was

selectively dissolved and removed from the blend. In case of PS-containing films, this was achieved by rinsing the sample with cyclohexane, which is a good solvent for PS²⁶ but does not dissolve doped PANI. In case of PMMA, the samples were rinsed with chloroform, which is a better solvent for PMMA than for PANI. The rinsing time was long enough to remove PMMA, but too short to dissolve PANI.

Optical micrographs were taken with a metallographic Nikon Epiphot 300 optical microscope. Dynamic Secondary Ion Mass Spectroscopy (dSIMS) measurements were performed using a VSW machine equipped with a liquid metal ion gun (FEI, Hillsboro, OR) and a quadrupole mass spectrometer (Balzers Instruments, Balzers, Liechtenstein). Both mapping and profiling modes of dSIMS were utilized. To calibrate the depth scale in these experiments, a series of test polymer thin films were prepared, whose thicknesses were first measured with an atomic force microscope (AFM). Further on, the samples were transferred into the dSIMS machine. Then, they were irradiated with the primary ion beam and the time needed to sputter away the whole thickness of the polymer film was recorded. AFM measurements were carried out with an Academia system microscope (Nanonics Imaging, Jerusalem, Israel) and with Agilent 5500 AFM. Both microscopes were working in noncontact mode.

The thickness of polymer composite films was measured by means of AFM. A scratch was made in the polymer film, revealing the silicon substrate and the gold layer. An AFM image was taken at the edge of the scratch from which the polymer film thickness could be determined.

RESULTS

UV-Vis Spectrum of the PANI(DBSA) Solution

PANI(DBSA) solution in xylene utilized in this study was characterized by means of UV-Vis spectroscopy. The absorption spectrum [Figure 2(a)] shows a peak at $\lambda = 300$ nm (designated as A), which can be attributed²⁷ to $\pi-\pi^*$ transitions in benzenoid rings. However, owing to strong absorption of the solvent below approx. 300 nm, this peak is not well resolved. That is why another measurement was performed for PANI(DBSA) dissolved in chloroform [Figure 2(b)]. The latter is transparent for light down to approx. 250 nm and as a result the band at $\lambda = 300$ nm is clearly visible. Two further peaks [Figure 2(a)] at $\lambda = 400$ nm (B) and $\lambda = 800$ nm (D) correspond to polaron band transitions. Moreover, a region of high absorbance for long wavelengths is present in the spectrum, with absorbance rising until the upper wavelength limit of the spectrometer, the effect characteristic of materials with metallic conductivity. It can be attributed to the straight conformation of macromolecules as mentioned in the **Introduction** section. Such behavior was also observed in certain cases by Xia et al.²⁸ for PANI(CSA) blends. It can be explained as a result of delocalization of polarons along a macromolecule and the smearing of the polar band. These factors lead to absorption in a wide range of wavelengths. Another suggestion of straight PANI(DBSA) conformation and charge delocalization comes from high dc conductivity of the films studied in this work (up to 7 S/cm, measured by the two-point technique). Moreover, in case of films manufactured from PANI(DBSA), a portion of not-doped PANI is present in the

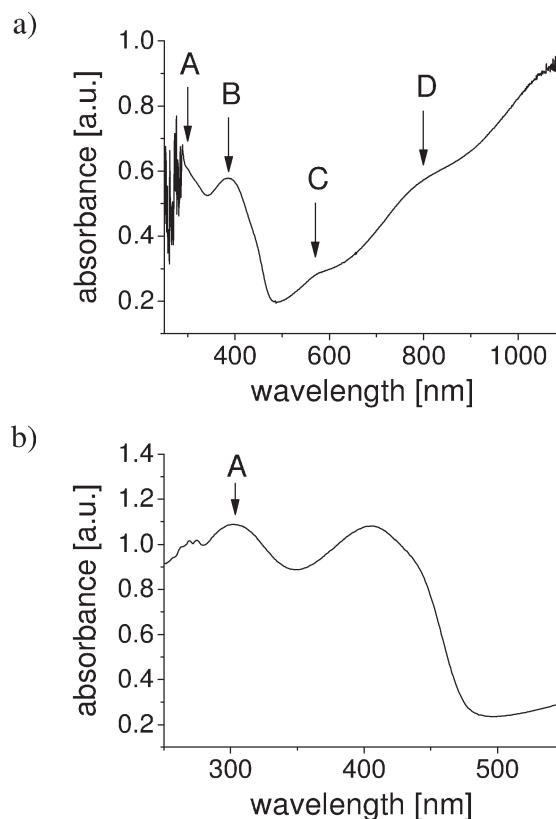


Figure 2. UV-Vis spectra of PANI(DBSA) dissolved in (a) xylene and (b) chloroform. Plot (b) is shown to present peak A more clearly, as it is not well resolved in (a) owing to UV absorption in xylene. Peak A corresponds to $\pi-\pi^*$ transitions in benzenoid rings in doped PANI, peaks B and D result from polaron band transitions, and peak C is caused by the presence of nondoped PANI (emeraldine base).

solution and, consequently, in the thin films. This fact is evidenced by the presence of an absorption peak close to $\lambda = 560$ nm [C in Figure 2(a)], attributed to emeraldine base.²⁷ Additionally, some amount of free DBSA is present in the film, which with its amphiphilic character (a hydrophobic alkyl chain on one end and a hydrophilic sulfonic group on the other) definitely has an effect on the phase separation process.

PANI(DBSA)/PS Films Spin-Cast in Dry Atmosphere

The surface of a PANI(DBSA)/PS film spin-cast in dry atmosphere from a xylene solution (total film thickness, approx. 570 nm) consists of numerous circular domains, with a diameter of approx. 1 μm , as seen in an optical micrograph [Figure 3(a)]. The modulus of a 2D Fast Fourier Transform calculated from the micrograph [Figure 3(a) inset, upper right] contains an isotropic ring, which testifies to the fact that there is no long-range order in the arrangement of domains. Radial average of the 2D FFT modulus (data not shown) has a peak at $k_{\text{max}} = 1.37 \mu\text{m}^{-1}$, and hence the average distance between the centers of neighboring domains is equal to $\langle r \rangle = 4.6 \mu\text{m}$. Chemical composition of domains was established using the mapping mode of SIMS. Circular domains are characterized by high intensity of secondary $^{26}\text{CN}^-$ ions [Figure 3(a), inset, lower right, bright contrast corresponds to high secondary ion intensity].

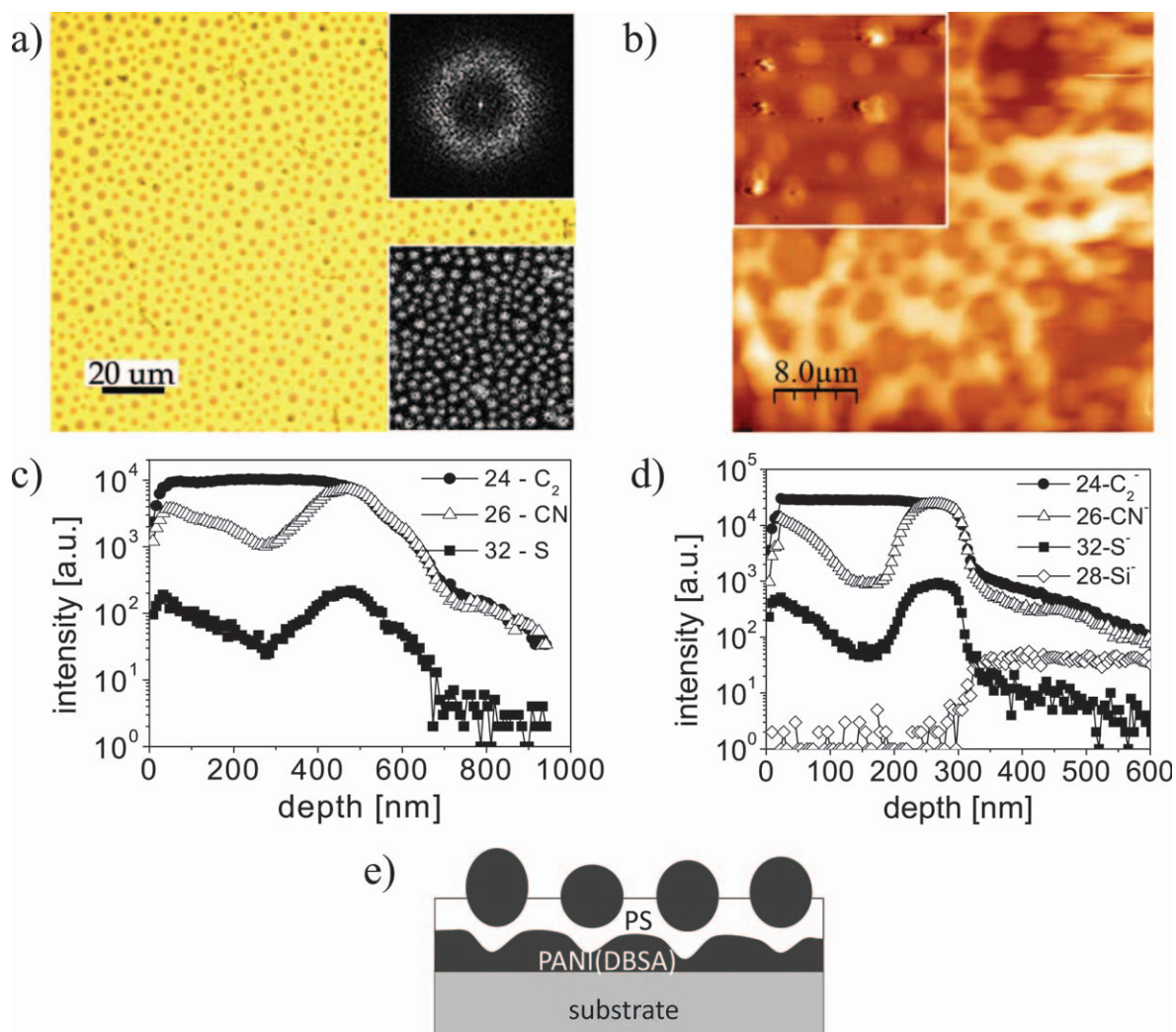


Figure 3. Thin PANI(DBSA)/PS film spin-cast in *dry* atmosphere from a solution containing 6 mg PANI(DBSA), 20 mg PS ($M_w = 125$ kDa) and 1 mL xylene. (a) Optical micrograph, its Fast Fourier Transform modulus (IFFT), inset, upper right), and a SIMS map (inset, lower right) of secondary $^{26}\text{CN}^-$ ions measured at an average depths of 21 nm, (b) AFM topographic map ($40 \times 40 \mu\text{m}^2$) of the sample after selective dissolution of PS and of raw sample ($20 \times 20 \mu\text{m}^2$, inset; different location); vertical scale is 1090 nm in the main image and 567 nm in the inset, (c) SIMS profiles (secondary ions indicated in the graph), (d) SIMS profiles of a sample spin-cast from the same solution in humid atmosphere (rel. humidity, $>90\%$), (e) model of the film morphology. [Color figure can be viewed in the online issue, which is available at wileyonlinelibrary.com.]

This fact proves that they are built of PANI, whereas adjacent regions are devoid of this polymer. A SIMS map of secondary $^{32}\text{S}^-$ ions (data not shown) measured in the same sample region directly after the first one (that is deeper in the sample) demonstrates that concentration of the dopant (DBSA) is high inside the domains. A SIMS profile of secondary ions within the sample depth [Figure 3(c)] shows a peak of PANI concentration close to the substrate, which means that besides circular domains the conjugated polymer forms a layer on the substrate as well. Topography of the sample was analyzed with an AFM [Figure 3(b), inset]. The measurement revealed that PANI(DBSA) domains are elevated above the average sample surface by approx. 100 nm. Another AFM image [Figure 3(b) main image, different location] taken after selective dissolution of PS (as described in the previous section), reveals a more

complicated microstructure: apart from circular domains, pores are observed in the polymer layer. This result combined with SIMS profiling clearly shows that PANI(DBSA) not only creates a layer on the substrate, but also forms circular domains in the film, which are separated from the PANI at the bottom by a PS-rich phase. Although the bottom layer is not changed on dissolution of the surrounding PS phase, the circular domains are removed from the sample during selective dissolution of PS, leaving pores behind.

Influence of Humidity on PANI(DBSA)/PS Film Morphology

Morphology of thin PANI(DBSA)/PS films spin-cast in humid atmosphere (other preparation conditions were not changed, total film thickness, approx. 300 nm) is similar to that of samples manufactured in dry atmosphere. Also, in this case circular

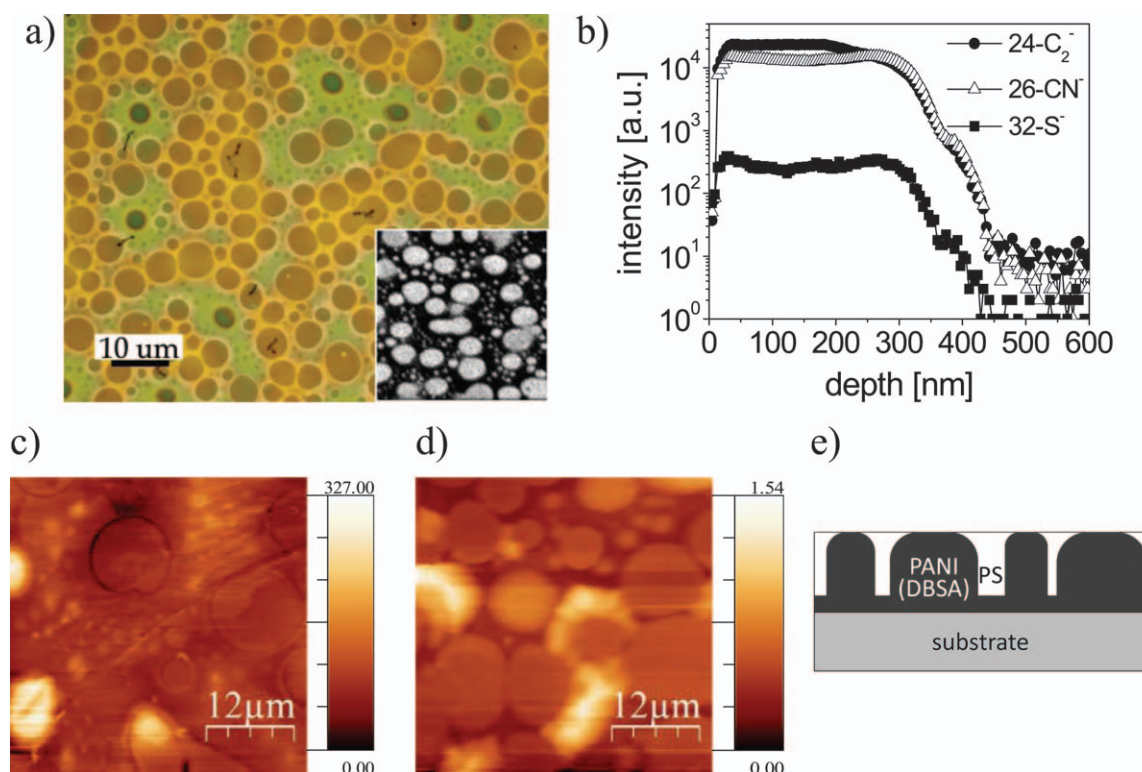


Figure 4. Thin PANI(DBSA)/PS film spin-cast in humid atmosphere (rel. humidity, >90%) from a solution containing 6 mg PANI(DBSA), 10 mg PS ($M_w = 125$ kDa) and 1 mL xylene. (a) Optical micrograph and a SIMS map (inset) of secondary $^{26}\text{CN}^-$ ions measured at an average depth of 23 nm, (b) SIMS profiles (secondary ions indicated in the graph), (c). AFM topographic map of raw sample; vertical scale is 327 nm, (d) AFM topographic map of the sample after selective dissolution of PS; vertical scale is 1540 nm., (e) model of the film morphology. [Color figure can be viewed in the online issue, which is available at wileyonlinelibrary.com.]

PANI(DBSA) domains are formed, arranged isotropically on the sample surface (data not shown). Also, here the domains are elevated above the surrounding PS phase; however, the average distance between domains is larger (radial average of FFT modulus yields $k_{\text{max}} = 1.12 \mu\text{m}^{-1}$, $\langle r \rangle = 5.6 \mu\text{m}$). High $^{32}\text{S}^-$ signal measured on domains in SIMS maps shows that the dopant (DBSA) is bound to PANI and there is no free DBSA in the PS phase. Also, in this case a layer rich in PANI close to the substrate is present, which is evidenced by a region of high nitrogen concentration above the substrate shown in Figure 3(d). Apparently, vertical phase separation in case of humid atmosphere is stronger than in case of dry conditions, as both edges of the $^{26}\text{CN}^-$ profile (that is near the substrate and the one facing the free surface) are much sharper here. Also, the Si^- profile showing the position of the substrate is sharp. The phase separation process is most probably influenced by humidity in the spin-coater chamber; however, as the sample manufactured in humid atmosphere is thinner than the one produced in dry conditions, the effect of sample thickness may also be important here.

PANI(DBSA)/PS Films with Reduced PS Content

Reducing PS content in the polymer blend (from 20 mg/mL in the solution to 10 mg/mL) results in a considerable change in morphology. Large PANI(DBSA) domains are formed, as evidenced by an optical micrograph [Figure 4(a)] and a SIMS map of $^{26}\text{CN}^-$ ions [Figure 4(a), inset] and $^{32}\text{S}^-$ ions (data not

shown). The edges of domains are sharp. Furthermore, a slight increase in $^{26}\text{CN}^-$ signal close to the substrate [by approx. a factor of 1.2, SIMS profile in Figure 4(b)] may suggest that there is a thin PANI(DBSA) layer on the substrate. AFM measurements performed on a fresh sample and after selective dissolution of PS [Figure 4(c, d)] demonstrate that solvent treatment does not generate pores in the films. It means that all PANI(DBSA) domains are attached directly to the substrate; in other words, the films do not contain PANI(DBSA) domains completely surrounded by PS. The total height of domains is approx. 250 nm, as measured with AFM. The overall film thickness can also be estimated from the SIMS profile by recording the sample depth at which the $^{24}\text{C}_2^-$ intensity starts to drop significantly. It should be emphasized that there is good agreement between this value (280 nm) and the value measured by AFM. Based on these results, one can propose the following model of film morphology in this case [Figure 4(e)]: a thin PANI(DBSA)-rich phase is situated on the substrate; this polymer also forms columns, surrounded by PS.

PANI(DBSA)/PMMA Films

Chemical nature of PMMA is different from that of PS. This difference can be expressed in terms of Hansen solubility parameters, which show affinity of chemical compounds as a function of the strength of dipole interactions, polar interactions, and hydrogen bonds in these compounds. PMMA is a polymer situated in the Hansen solubility parameter space at some

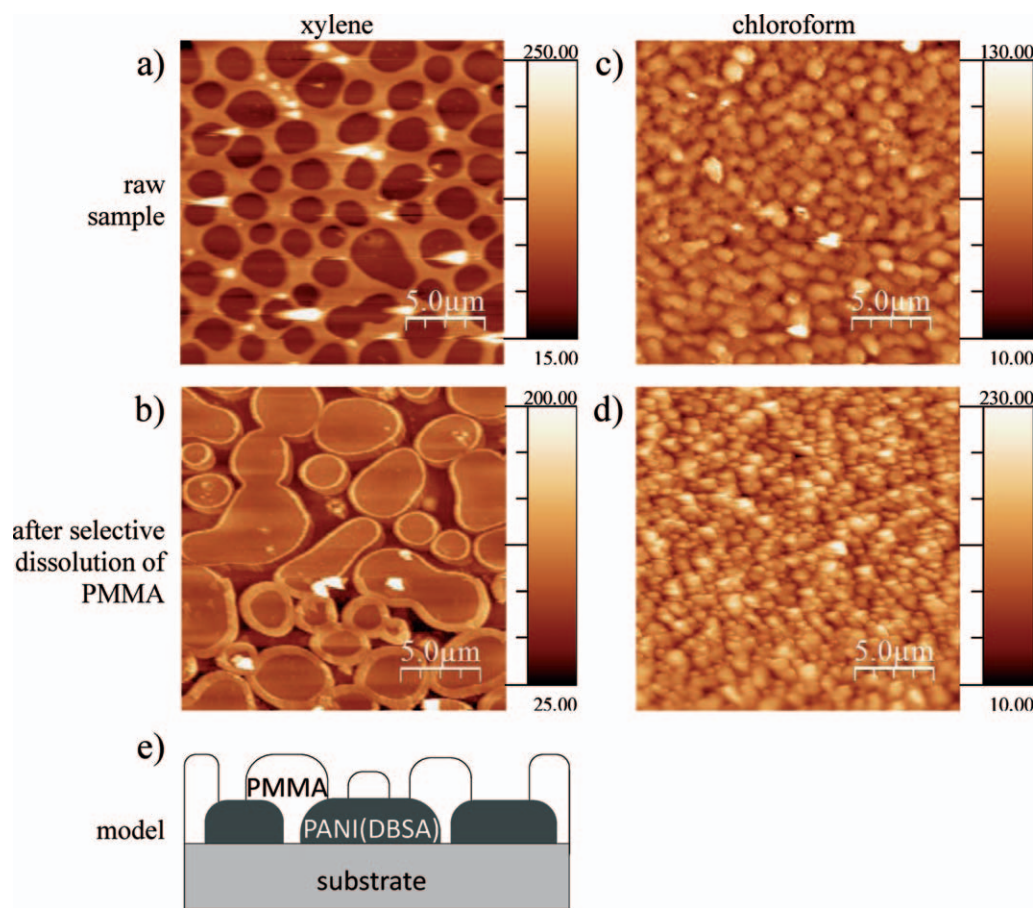


Figure 5. (a–d) AFM topographic images of a thin PANI(DBSA)/PMMA film spin-cast in dry atmosphere from a solution containing 6 mg PANI(DBSA), 10 mg PMMA ($M_w = 14.4$ kDa) and 1 mL xylene (a–b) or 1 mL chloroform (c, d); images were taken on raw samples (a and c) and after selective dissolution of PMMA (b and d); vertical scale is in nm, (e) morphological model of the film spin-cast from xylene solution. [Color figure can be viewed in the online issue, which is available at wileyonlinelibrary.com.]

distance with respect to PS ($D_{PS-PMMA} = 6.3 \text{ MPa}^{1/2}$).²⁶ As a result, these two polymers lead to different morphological structures when mixed with doped PANI. In a thin PANI(DBSA)/PMMA film manufactured by spin coating in humid atmosphere from a xylene solution (with PANI(DBSA) : PMMA ratio of 6 : 10 by weight), circular and elongated domains with lateral size up to approx. 4 μm are visible [AFM topographic map, Figure 5(a)]. These domains are considerably larger than in the case of the PANI(DBSA)/PS film with the same polymer weight ratio (6 : 10). Similarly to the case of PANI(DBSA)/PS blends, the domains are built of PANI. This is again evidenced by SIMS maps (data not shown), displaying high $^{26}\text{CN}^-$ signal inside these domains, which attests to high PANI concentration. Moreover, the domains are left intact after selective dissolution of PMMA, whereas the surrounding phase is washed away [AFM topographic map, Figure 5(b)]. This yet again proves that the domains are built of PANI. Furthermore, the domains are 70 nm lower than the PMMA phase. Morphology of a sample prepared from the same solution, but spin-cast in humid atmosphere is qualitatively the same—apparently water vapor does not influence morphology of the film, in contrast to composites containing PS.

Influence of Solvent on the Final Morphology

The solvent strongly influences morphology of the films. In a PANI(DBSA)/PMMA mixture, changing the solvent from xylene to much more volatile chloroform (vapor pressures at 20°C equal to 12 and 213 hPa, for xylene and chloroform, respectively) leads to granular morphology. The domain diameter is approx. 1 μm and their height approx. 40 nm [AFM topographic map, Figure 5(c)]. The roughness of the sample in this case is equals to $\sigma_{\text{rms}} = 14.6$ nm. AFM images taken after selective dissolution of PMMA [Figure 5(d)] show that PANI domains (with height of 100 nm) are not removed during solvent treatment. This result indicates that the domains are densely arranged on the substrate and are bound to it.

Thin PANI(DBSA)/PS films spin-cast from chloroform in humid atmosphere (data not shown) are much smoother ($\sigma_{\text{rms}} = 7.9$ nm) and a characteristic feature of their morphology is the presence of small (diameter, <300 nm) pores. Moreover, during selective dissolution of PMMA, a large portion of polymeric material is removed, leaving polymer aggregates on smooth Au substrate. It means that in this composite material some PANI(DBSA) domains are attached to the substrate, whereas others grow during spin coating in the sample bulk.

DISCUSSION

The formation process of PANI(DBSA)/PS films with high PS content (20 mg/mL in the solution) may be described as follows: in the initial stage of spin coating, a PANI(DBSA)-rich layer develops on the substrate as a result of strong specific interaction of PANI with gold. A PS-rich layer is situated above. Further on, undulations of the polymer interface develop, which grow in amplitude and finally lead to PANI(DBSA) droplets in the PS phase, detached from the PANI(DBSA) layer at the bottom, as shown in a model picture in Figure 3(e). DBSA present in the droplets enhances droplet breakup and inhibits their recoalescence (a mechanism described by Baret et al.²⁹). This is in agreement with SIMS profiling results [Figure 3(c)]: high concentration of $^{26}\text{CN}^-$ ions near the free surface (depth, close to 0 nm in the dSIMS profile) corresponds to PANI(DBSA) circular domains. The reduction of nitrogen concentration deeper in the sample corresponds to the PS layer, separating droplets from PANI(DBSA) at the bottom, whereas the peak in $^{26}\text{CN}^-$ concentration appears when the primary ion beam sputters away the bottom PANI(DBSA) layer.

In case of PANI(DBSA)/PS composites, the difference in size of PANI(DBSA) domains between the samples prepared in dry and in humid atmosphere can be explained in the following way: PANI, a hygroscopic component of the mixture, absorbs water from the spin-coater chamber, which leads to the swelling of this polymer. The effect of water absorption in PANI was observed and studied, for example, by Matveeva et al.³⁰ During the film formation, long alkyl chains of DBSA chemically bound to PANI are directed toward the hydrophobic PS phase and outside PANI(DBSA) domains. Also, excess DBSA, not chemically bound to PANI, is situated at domain borders, acting as a surfactant. Such behavior of free DBSA has been reported in the literature, for example, by Barra et al.³¹ for mixtures of PANI(DBSA) and ethylene–vinyl acetate copolymer. As a result, water molecules are trapped inside domains, which remain swollen till the last stages of thin film formation. In consequence, PANI(DBSA) domains are larger in samples prepared in humid atmosphere than in dry conditions.

Reducing matrix polymer (PS) content in the solution from 20 to 10 mg/mL leads to PANI(DBSA) domains that are connected with the bottom PANI(DBSA) layer. In this case, the PS content is too small to produce a continuous layer between these PANI(DBSA)-rich regions.

As mentioned before, morphology of thin polymer films containing PMMA is much different from that of the films with PS. PMMA is a hydrophilic polymer, with considerably higher Hansen parameter for hydrogen bond formation ($\delta_H = 7.5 \text{ MPa}^{1/2}$) than PS ($\delta_H = 4.3 \text{ MPa}^{1/2}$).²⁶ Alkyl chains of DBSA molecules situated close to domain surfaces render these surfaces hydrophobic. As a result, domains are poorly wetted by the hydrophilic PMMA phase. This in turn leads to complete or partial dewetting of PANI(DBSA) domains, leaving these domains exposed with a continuous PMMA phase surrounding them.

Experimental data of thin films spin-cast from a chloroform solution show that in case of this solvent polymer domains in the final samples are relatively small. Additionally, films spin-cast in

humid atmosphere are porous. The former effect is connected with the kinetics of drying. In case of xylene solutions, long drying time allows for the formation of large PANI(DBSA) domains in the process of coalescence. In contrast, in a chloroform solution the solvent rapidly escapes from the film as a result of its high vapor pressure, blocking the diffusion of PANI. Porosity of films, in turn, can be explained similarly to a discussion presented by Cui et al.³² in which authors studied the mixtures of PS and poly(2-vinylpyridine). The phenomenon is namely the effect of water condensation on the solution surface, which is cooled down by rapid evaporation of the solvent. Water droplets create depressions on the solution surface with diameter of $<1 \mu\text{m}$. Because of relatively low vapor pressure, water only evaporates from the surface when the film is already solid, which leads to pores observed in the AFM images. Water does not condensate on the surface of xylene solution, as there is no considerable decrease in surface temperature owing to low evaporation rate of this solvent. A similar effect—the formation of porous films in humid atmosphere containing PANI(DBSA) and nanoparticles of Fe_3O_4 —has been reported by Yu et al.³³

It should also be mentioned here that according to SIMS measurements, dopant molecules are always present in PANI domains regardless of atmospheric humidity during spin coating. This is evidenced by $^{32}\text{S}^-$ profiles, which have the same shape as $^{24}\text{CN}^-$ profiles [Figures 3(c, d) and 4(b)]. This behavior is in contrast with thin composite films containing PANI(CSA), in which case in the presence of water vapor the dopant migrates toward the free surface.³⁴

CONCLUSIONS

Morphology of thin polymer films containing PANI(DBSA) and a conventional polymer (PS or PMMA) is strongly influenced by the PANI dopant (DBSA). In the final film, there is a portion of DBSA that is not chemically bound with PANI. Because of the amphiphilic character of the acid, PANI(DBSA) domains are formed with long alkyl chains of the dopant directed outside the domains. DBSA acting as a surfactant prevents droplet coalescence during blend film formation. Furthermore, water vapor influences domain formation in case of strongly hydrophobic PS. In this instance, water molecules are trapped inside domains, which, as a consequence, are swollen with respect to the ones in dry atmosphere. No influence of water vapor is observed in case of PANI(DBSA)/PMMA mixtures. Changing the solvent from xylene to a much more volatile chloroform results in smaller domains owing to shorter drying time of these films. Moreover, spin coating a polymer solution in this solvent in humid atmosphere leads to the formation of submicron pores on the sample surface, most probably resulting from water vapor condensation on the solution surface. Another effect observed here is that circular PANI(DBSA) domains are smaller in a PANI(DBSA)/PMMA 6 : 10 film than in the PANI(DBSA)/PS 6 : 10 film.

ACKNOWLEDGMENTS

This work was partially financed by the Polish Ministry of Science and Higher Education from funds allotted to science in 2010.

REFERENCES

1. Cao, Y.; Smith, P.; Heeger, A. *Synth. Met.* **1992**, *48*, 91.
2. Clark, N. B.; Maher, L. J. *Funct. Polym.* **2009**, *69*, 594.
3. Steffens, C.; Manzoli, A.; Francheschi, E.; Corazza, M. L.; Corazza, F. C.; Vladimir Oliveira, J.; Herrmann, P. S. P. *Synth. Met.* **2009**, *159*, 2329.
4. Wojkiewicz, J. L.; Bliznyuk, V. N.; Carquigny, S.; Elkamchi, N.; Redon, N.; Lasri, T.; Pud, A. A.; Reynaud, S. *Sens. Actuat. B Chem.* **2011**, *160*, 1394.
5. Deore, B.; Diaz-Quijada, G. A.; Wayner, D.D. M.; Stewart D.; Won D.; *Waldron P. ECST* **2011**, *35*, 83.
6. Radhakrishnan, S.; Rao, C.R. K.; Vijayan, M. J. *Appl. Polym. Sci.* **2011**, *122*, 1510.
7. Chang, Mei-Ying; Wu, Chong-Si; Chen, Yi-Fan; Hsieh, Bi-Zen; Huang, Wen-Yao; Ho, Ko-Shan; Hsieh, Tar-Hwa; Han, Yu-Kai *Org. Electron.* **2008**, *9*, 1136.
8. Fan, B.; Castro, F.A. D.; Chu, B.T. T.; Heier, J.; Opris, D.; Hany R.; Nuesch, F. J. *Mater. Chem.* **2010**, *20*, 2952.
9. Schettini, A.R. A.; Soares, B. G. *Macromol. Symp.* **2011**, *299/300*, 164.
10. Das, C. K.; Mandal, A. *J Mater. Sci. Res.* **2012**, *1*, 45.
11. Cristovan, F. H.; Pereira, E. C. *Synth. Met.* **2011**, *161*, 2041.
12. Gonçalves, G. S.; Baldissera, A. F.; Rodrigues L. F.; Martini, E.M. A.; Ferreira, C. A. *Synth. Met.* **2011**, *161*, 313.
13. Barros, R. A.; Martins, C. R.; Azevedo, W. M. *Synth. Met.* **2005**, *155* 35.
14. Lenhart, N.; Crowley, K.; Killard, A. J.; Smyth, M. R.; Morrin, A. *Thin Solid Films* **2011**, *519*, 4351.
15. Haberko, J.; Raczowska, J.; Bernasik, A.; Rysz, J.; Nocuń, M.; Nizioł, J.; Łuźny, W.; Budkowski, A. *Mol. Cryst. Liquid Cryst.* **2008**, *485*, 796.
16. Österholm, J. E.; Cao Y.; Klavetter F.; Smith, P. *Polymer* **1994**, *35*, 2902.
17. Han, Y.; Kusunose, T.; Sekino, T. *Synth. Met.* **2009**, *159*, 123.
18. Su, Shi-Jian; Kuramoto, N. *Synth. Met.* **2000**, *108*, 121.
19. Soares, B. G.; Celestino, M. L.; Magioli, M.; Moreira, V. X.; Khastgir, D. *Synth. Met.* **2010**, *160*, 1981.
20. Bhadra, S.; Khastgir, D.; Singha, N. K.; Lee, J. H. *Prog. Polym. Sci.* **2009**, *34*, 783.
21. Chua, L.-L.; Ho, P.K. H.; Sirringhaus, H.; Friend, R. H. *Adv. Mater.* **2004**, *16*, 1609.
22. Corcoran, N.; Arias, A. C.; Kim, J. S.; MacKenzie, J. D.; Friend, R. H. *Appl. Phys. Lett.* **2003**, *82*, 299.
23. Segal, E.; Tchoudakov, R.; Narkis, M.; Siegmann, A.; Wei, Y. *Sens. Actuat. B* **2005**, *104*, 140.
24. Vicentini, D. S.; Barra, G.M. O.; Bertolino, J. R.; Pires, A.T. N. *Eur. Polym. J.* **2007**, *43*, 4565.
25. Basavaraja, C.; Kim, W. J.; Kim, D. G.; Huh, D. S. *Polym. Comp.* **2012**, *33*, 388.
26. Mark, J. E. *Polymer Data Handbook*; Oxford University Press: New York, **1999**.
27. Yin, W.; Ruckenstein, E. *Synth. Met.* **2000**, *108*, 39.
28. Xia, Y.; Wiesinger, J.; MacDiarmid, A.; Epstein, A. *Chem. Mater.* **1995**, *7*, 443.
29. Baret, J.-C.; Kleinschmidt, F.; El Harrak, A.; Griffiths, A. D. *Langmuir* **2009**, *25*, 6088.
30. Matveeva, E. S.; Diaz Calleja, R.; Parkhutik, V. P. *Synth. Met.* **1995**, *72*, 105.
31. Barra, G.M. O.; Leyva, M. E.; Soares, B. G.; Sens. M. *Synth. Met.* **2002**, *130*, 239.
32. Cui, L.; Peng, J.; Ding, Y.; Li, X.; Han, Y. *Polymer* **2005**, *46*, 5334.
33. Yu, C.; Zhai, J.; Li, Z.; Wan, M.; Gao, M.; Jiang, L. *Thin Solid Films* **2008**, *516*, 5107.
34. Bernasik, A.; Haberko, J.; Włodarczyk-Miśkiewicz, J.; Raczowska, J.; Łuźny, W.; Budkowski, A.; Kowalski, K.; Rysz, J. *Synth. Met.* **2005**, *155*, 516.